

# The role of co-circularity of local elements in texture perception

Isamu Motoyoshi

Human and Information Science Laboratory,  
NTT Communication Science Laboratories,  
NTT, Atsugi, Japan



Frederick A. A. Kingdom

McGill Vision Research Unit, McGill University,  
Montreal, Quebec, Canada



The present study analyzes the effect of local pairwise orientation relations on the perception of textural structure. We have employed a new class of stochastic stimuli comprised of paired Gabor patches with a particular orientation difference ( $\theta$ ) and relative angular position ( $\phi$ ). We measured the threshold proportion of signal pairs for discriminating the target texture from a noise texture comprised of randomly oriented pairs. The results showed that observers were sensitive not only to textures containing pairs with curvilinear configurations such as lines and curves ( $\phi = \theta / 2$ ), but also to their orthogonal configurations such as V shapes and parallels ( $\phi = \theta / 2 + 90$ ). Both classes of configuration exhibit the property of co-circularity, a fundamental geometric feature of edges and contours in natural images. We also found higher sensitivity for textures made from orientation pairs with either large or small orientation differences. These results suggest that in addition to orientation difference, co-circularity plays a critical role in the perception of orientation-based textural structure.

Keywords: texture, orientation, co-circularity

Citation: Motoyoshi, I., & Kingdom, F. A. A. (2010). The role of co-circularity of local elements in texture perception. *Journal of Vision*, 10(1):3, 1–8, <http://journalofvision.org/10/1/3/>, doi:10.1167/10.1.3.

## Introduction

A number of psychophysical studies of human texture perception support the idea that the segmentation and discrimination of texture regions is based on the detection of differences in simple image features such as element orientation, size, or spatial frequency (Arsenault, Wilkinson, & Kingdom, 1999; Dakin & Watt, 1997; Graham, Beck, & Sutter, 1992; Julesz, 1981; Kingdom, Keeble, & Moulden, 1995; Landy & Bergen, 1991; Nothdurft, 1985; Wolfson & Landy, 1998). Differences in orientation, as well as other features, are believed to be detected by Energy or Filter–Rectify–Filter mechanisms (Bergen & Adelson, 1988; Landy & Bergen, 1991; Malik & Perona, 1990). Physiological evidence also supports the existence of neurons sensitive to orientation differences in texture patterns (Knierim & van Essen, 1992; Zipser, Lamme, & Schiller, 1996).

On the other hand, several studies on texture perception have considered the role of higher order statistics in the form of *spatial correlations* between texture elements, either in terms of position or orientation. In his early studies of texture segmentation, Julesz argued for the importance of second-order texture statistics, which are measurements of the relations among pairs, or dipoles, of *pixels* (Julesz, Gilbert, Shepp, & Frisch, 1973). In later work Julesz placed more emphasis on a class of local

features termed “textons,” examples of which are T and L shapes (Julesz, 1981). Ls and Ts can be considered examples of pairwise relations, not among pixels but among *oriented elements*. More recently, the role of spatial relations among neighboring elements in texture perception has been revealed through studies of texture *appearance*. For example, local curvature and continuity of orientation have been shown to be critical to the structural appearance of textures that are characterized by systematic variations in local orientation (Ben-Shahar, 2006; Ben-Shahar & Zucker, 2004; Claessens & Wagemans, 2005). Furthermore, studies on texture synthesis, which attempt to determine the statistical properties that best capture the appearance of natural textures, have also revealed the importance of local spatial relations among texture elements (Heeger & Bergen, 1995; Portilla & Simoncelli, 2000).

The most extensive investigations of the significance of spatial relations among oriented elements have not however been made in the context of texture perception but in the context of contour detection in noise (Field, Hayes, & Hess, 1993; Hess & Dakin, 1997; May & Hess, 2008). In the contour detection studies, observers are asked to detect “path(s)” made of locally aligned elements among randomly oriented elements. The observers’ performance systematically depends on the orientation difference between neighboring elements and the between-element separation, with best performance when the target

elements are collinear and closely spaced. These results have been interpreted as manifestations of neural mechanisms that integrate orientation signals that have collinear or co-curvilinear configurations (Kapadia, Ito, Gilbert, & Westheimer, 1995; Polat, Mizobe, Pettet, Kasamatsu, & Norcia, 1998; Polat & Sagi, 1993). Configurations of orientations of even higher order have been investigated using “global form” stochastic stimuli such as glass patterns and patterns with mirror symmetry (Barlow & Reeves, 1979; Claessens & Wagemans, 2008; Glass, 1969; Locher & Wagemans, 1993; Wagemans, Van Gool, Swinnen, & Van Horebeek, 1993; Wilson & Wilkinson, 1998).

In the present study, we examine the role of relations among oriented elements in the perception of textural structure using a parameter space that is much more extensive than the one represented either in Julesz’s textons or the contour detection studies. To this end, we have developed a novel class of artificial texture stimulus, examples of which are shown in Figure 1a. The textures comprise large numbers of pairs of adjacent Gabor elements. Each pair of Gabor patches has a particular orientation difference  $\theta$  and a particular relative angular position  $\phi$ . The absolute orientation of each pair is however random. As demonstrated in Figure 1a, the textures vary in appearance depending on the combination of these two parameters. While some parameter combinations produce textures that appear very different from the random-pair texture shown in the upper left, others do not.

Figure 1b illustrates the signal pairs arranged in a 2D space of orientation difference ( $\theta$ ) and relative angular position ( $\phi$ ). In this space, when  $\phi = \theta / 2$  or  $\phi = \theta / 2 + 90$ , the element pairs are “co-circular,” that is, the two oriented elements are tangent to ( $\phi = \theta / 2$ ), or radial along ( $\phi = \theta / 2 + 90$ ), a common circle. In Figure 1c, we have transformed the space of element pairs into the dimensions of orientation difference  $\theta$  and co-circularity  $\chi = \theta / 2$ , the latter denoted from now on as  $\chi$ . In this space, the pairs at  $\chi = 0$  deg (these are the pairs in the leftmost column in Figure 1c, which include those with a  $\theta$  of 90 deg that are strictly speaking neither tangent to nor radial along a common circle) constitute tangent-type co-circularity while those at  $\chi = 90$  deg constitute radial-type co-circularity (the pairs in the rightmost column in Figure 1c). Using these textures, we have examined the threshold proportion of signal pairs required to discriminate the texture from “noise”. The noise comprised all possible types of the pairs shown in the space of Figures 1b and 1c.

We expected that sensitivity would be highest for textures defined by collinear pairs ( $\chi$  and  $\theta$  are both 0 deg) with sensitivity declining rapidly with orientation difference  $\theta$  (as expected from the contour detection studies). However, we found that observers retained high sensitivities for tangent-type co-circular pairs ( $\chi = 0$  deg) across a

wide range of orientation difference  $\theta$ , with sensitivity peaking for curvilinear pairs with  $\theta = 45$  deg rather than collinear pairs ( $\theta = 0$ ). Moreover, observers were sensitive not only to tangent-type co-circular pairs but also to pairs that were radial-type co-circular, that is, parallels or V shapes where  $\chi$  is close to 90 deg. These results suggest that co-circularity rather than collinearity is the critical variable in the perception of structure in texture regions.

## Methods

### Apparatus

Images were generated by a graphics card (CRS VSG2/5 or ViSage) and displayed on a 21-inch CRT (SONY GDM F500R) with a luminance resolution of 8 bits. The viewing distance was 1.25 m. The mean luminance of the background was 40 cd/m<sup>2</sup>.

### Subjects

Two naive subjects (TL, YI; not researchers) and the authors (IM, FK) with corrected-to-normal vision participated the experiment. The data for IM and FK were collected in 2004, but for the others the data were collected in 2008. All the experiments were approved by the NTT Ethics Committee with completed consent forms.

### Stimuli

The stimulus was a circular texture field of 8.25 deg diameter that consisted of  $\sim 183$  pairs of Gabor patches (Figure 1). Each Gabor pattern was a sinusoidal grating with a spatial frequency of 7.3 c/deg windowed by a Gaussian with a standard deviation of 0.07 deg. It had a luminance contrast of 0.8 and random spatial phase. Each pair of Gabor patches was separated by a fixed center-to-center distance of 0.28 deg. The pairs were randomly placed within the texture field under the constraint that the center-to-center separation between adjacent pairs was a minimum of 0.41 deg; hence neither the elements nor the element pairs ever overlapped. Each texture contained a certain proportion of “signal” and “noise” pairs. In each “signal” pair, one Gabor was located at a particular angular position ( $\phi$ , 0–165 deg) and orientation ( $\theta$ , 0–90 deg) relative to the other element. Both were varied in 15 deg steps, resulting in a total of  $12 \times 7 = 84$  different pairs. The absolute orientation of one element was random. Each pair was randomly mirrored. In the “noise” pairs, the two parameters were randomly set for

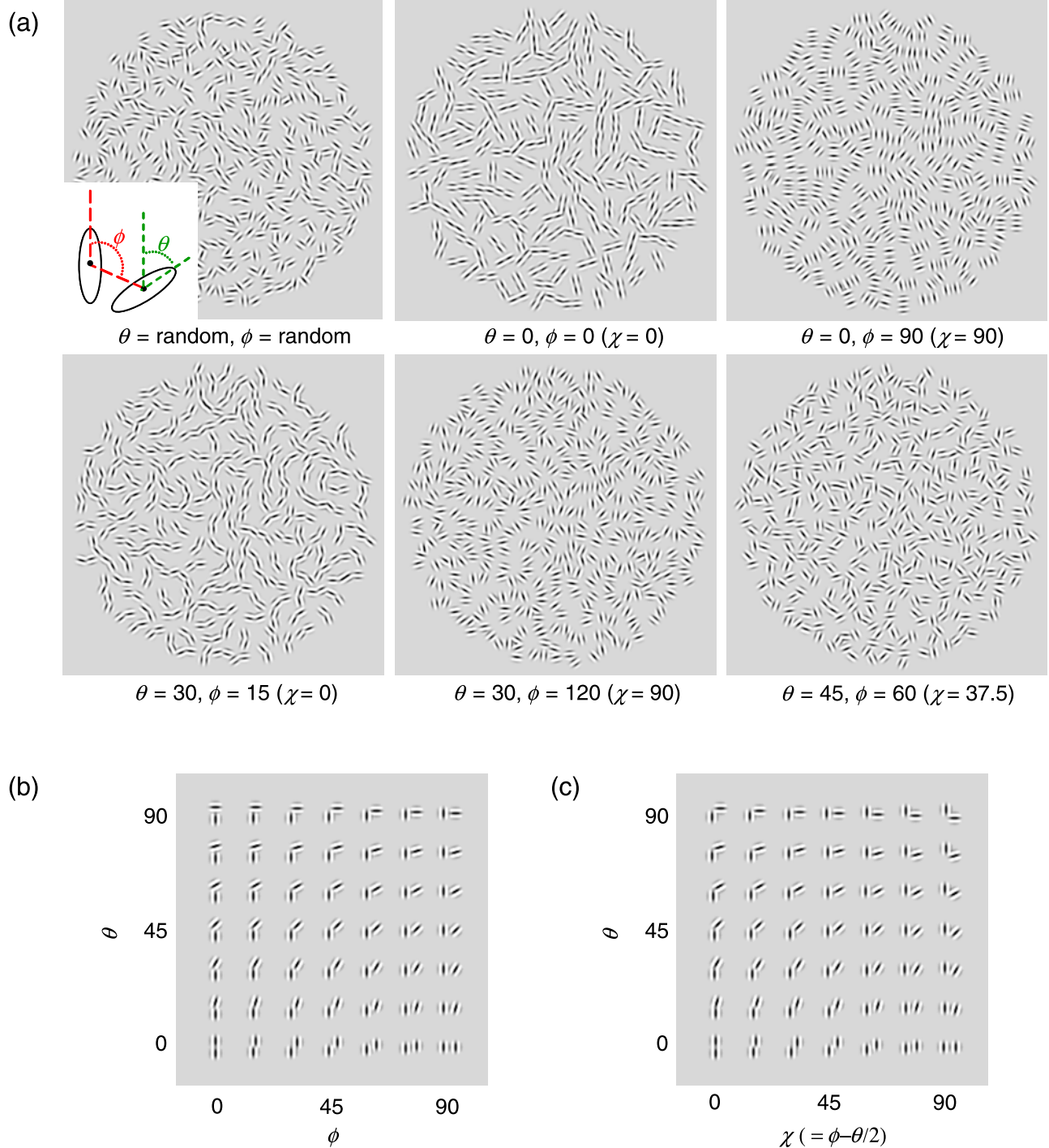


Figure 1. (a) Examples of stimuli used in the experiment. All textures shown here contain 100% signal pairs except for the random-pair texture in the upper left. Each pair of Gabor patches is defined by a particular orientation difference ( $\theta$ ) and angular position ( $\phi$ ). (b) Signal pairs in each condition are arranged in a space of  $\phi$  and  $\theta$ . (c) Signal pairs are arranged in a transformed space of  $\chi (= \phi - \theta/2)$  and  $\theta$ , in which the pairs are co-circular when  $\chi = 0$  deg (tangent) and when  $\chi = 90$  deg (radial).

each individual pair. In other words the noise pairs were constructed and positioned according to the same principles as the signal pairs except that the orientation and positional relations between the elements of each pair were random.

Before conducting the main experiment, the authors phase scrambled all the textures using Fourier and inverse Fourier transformations and observed that, provided the phases of the Gabor patches were randomized, they were all indiscriminable.

## Procedure

Using a two-interval forced choice (2IFC) procedure with an interleaved staircase, we examined threshold signal% for discriminating the target from a noise texture. Subjects were shown in advance all varieties of target texture and became accustomed to the idea that the target textures had various types of structure. On each trial, the target and noise textures were presented in random order for 500 ms each with a blank field of 670 ms. Subjects were asked to indicate by button press the target texture. They were instructed to judge on the basis of the global impression of the texture, and most observers reported choosing the texture that appeared more structured. An incorrect response was followed by a tone. The proportion of “signal pairs” in each condition was decreased by 0.1 log unit after two correct responses and increased by the same amount after one incorrect response. All 84 conditions were randomly interleaved in a session. Data for geometrically equivalent conditions, for example,  $(\theta, \phi) = (90, 0)$  and  $(90, 90)$ , were pooled in the analysis. On average the whole session took  $\sim 7500$  trials, but subjects were allowed to take a break every  $\sim 600$  trials. At the end of the session, the thresholds at the 75% correct level, as well as their standard errors, were calculated by maximum likelihood estimation and bootstrapping (5000 samples). For conditions in which the target texture of

100% signal pairs did not reach 75% correct, the threshold was defined as 100%.

## Results

Figure 2 shows sensitivities, defined as  $100 / \text{threshold signal \%}$ , as a function of the relative angular position  $\phi$  in the signal pair. Each panel shows results for a different orientation difference  $\theta$ . Observers are clearly sensitive only to textures with specific combinations of  $\phi$  and  $\theta$ .

The sensitivity functions exhibit a characteristic clover-leaf shape. The first pole of the clover leaf (going clockwise from  $\phi = 0$ ) occurs when  $\phi$  is half of  $\theta$  (i.e.,  $\phi = \theta / 2$ ) as denoted by a red arrow. The second pole, which is smaller in magnitude but still pronounced, occurs at the orthogonal orientation of the first pole (i.e.,  $\phi = \theta / 2 + 90$ ), as denoted by a green arrow. These poles indicate that subjects are especially sensitive to pairs with a co-circular configuration in the space of Figure 1c. The first pole is for pairs that are tangent to the circle, i.e., form smooth curves, while the second pole is for pairs that are radial along the circle, i.e., form sharp curves such as V shapes. However the cloverleaf-shaped sensitivity curve is markedly reduced when  $\theta$  is close to parallel (0 and 15 deg)

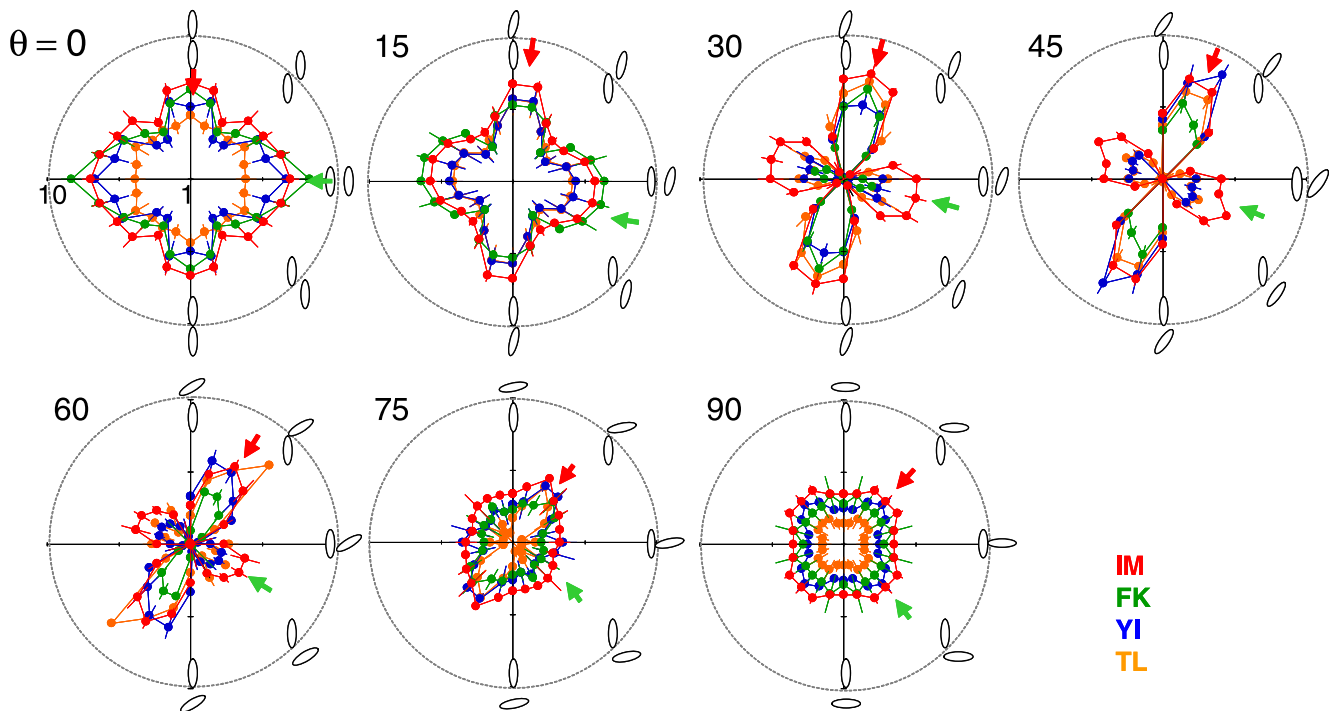


Figure 2. Results of the experiment. (a) Polar plots are log sensitivity ( $100 / \text{threshold signal \%}$ ) as a function of the relative angular position  $\phi$ . Each panel shows the results for a different orientation difference  $\theta$ . Small ellipses illustrate the signal pairs. Red arrows denote the condition in which  $\phi = \theta / 2$  ( $\chi = 0$ ), and green arrows  $\phi = \theta / 2 + 90$  ( $\chi = 90$ ). Different colors represent different subjects. Error bars represent  $\pm 1$  SEM.



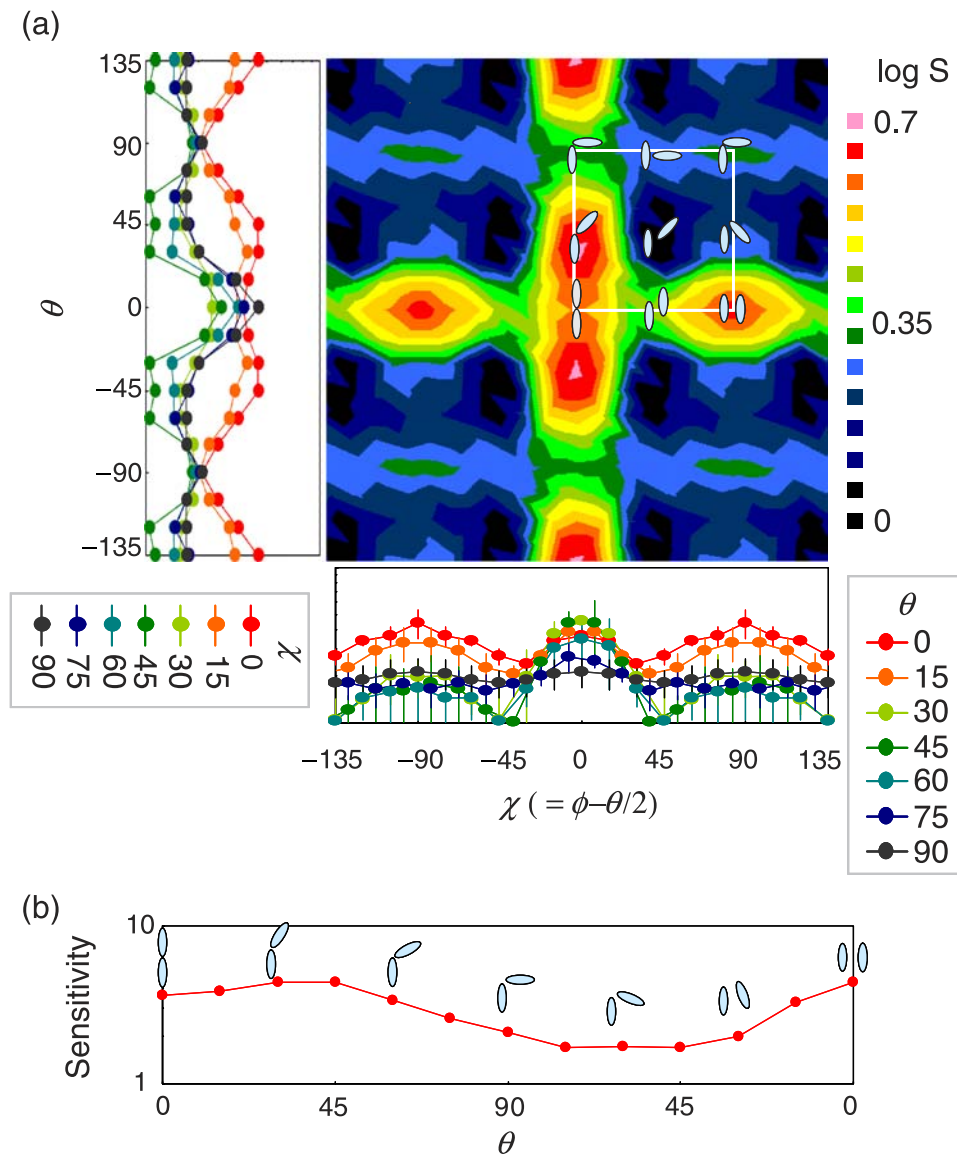


Figure 3. (a) Average log-sensitivity data across observers plotted in a 2D plane of  $\chi$  and  $\theta$ . The region denoted by white lines corresponds to the  $\chi$ - $\theta$  space shown in Figure 1c. Line plots for both axes are also shown. (b) Average sensitivity for co-circular pairs as a function of angle  $\theta$ . The left side of the plot indicates the data for the tangent-type co-circular pairs ( $\chi = 0$  deg), and the right side for the radial-type co-circular pairs ( $\chi = 90$  deg).

and almost absent when close to orthogonal (75 and 90 deg).

To visualize these tendencies more easily, Figure 3a plots the data averaged across subjects in a 2D plot that is a function of  $\chi$  and  $\theta$ , together with the line plots for each dimension. The line plot against  $\chi$  clearly shows two peaks in sensitivity, one at  $\chi = 0$  deg (tangent co-circular) and the other at  $\chi = 90$  deg (radial co-circular), but no clear peak is found when  $\theta$  is 75 and 90 deg (orthogonal). The line plot against  $\theta$  also shows two peaks with regard to the orientation difference ( $\theta$ ), one at 0 deg (parallel) and the other at 90 deg (orthogonal), but not for pairs with small  $\chi$ s of 0 and 15 deg (tangent-type co-circular). In these conditions, sensitivity declines at a  $\theta$  of 90 deg (and

also slightly at a  $\theta$  of 0 deg). The other tendency revealed in these plots is that sensitivity is generally high when  $\chi$  is 0 or 15 deg (red and orange lines in both plots), but this reflects the fact that the first peak in sensitivity, which occurs at around 0 deg in each variable, is more profound than the second one, which occurs at 90 deg.

Overall, the 2D plot appears like a lattice of overlapping vertical and horizontal gratings, each consisting of two ridges, large in the center and small at the sides. Sensitivity appears to vary almost independently along the dimensions of  $\chi$  and  $\theta$ , i.e., of co-circularity and orientation difference.

Figure 3b plots the data along the two ridges that represent the data from the tangent-type ( $\chi = 0$  deg, left half) and radial-type ( $\chi = 90$  deg, right half) co-circular

pairs. The plot shows that sensitivity for co-circular pairs varies with angle but never drops to one.

## Discussion

In the present study, we systematically explored the pairwise relations of oriented elements that determined the discriminability of orientation-defined texture regions. While different pairwise orientation relations produced textures with markedly different appearance, their discriminability from random-pair noise textures showed a systematic dependency on co-circularity ( $\chi$ ) and orientation difference ( $\theta$ ); observers were especially sensitive to textures that contained co-circular pairs and pairs with either small or large orientation differences.

At a qualitative level, it could be said that observers were most sensitive to textures comprised of signal pairs that form straight lines, smooth curves, parallel lines, V shapes, L shapes, and T shapes. These features are similar to the classical list of “textons” proposed by Julesz (1981) for texture segmentation. This may indicate that neural mechanisms sensitive to textons play a role in the discrimination of our textures. However, there is no clear evidence to date for the existence of specific texton detectors in the visual system.

On the other hand, the regularities in the present data lead to a simpler explanation, but one different from that argued to underpin the results from contour detection studies where collinearity has been shown to be the critical feature (Field et al., 1993; Hess & Dakin, 1997). While a collinearity-sensitive mechanism is consistent with our finding that observers are particularly sensitive to tangent-type co-circular pairs ( $\chi$  close to 0 deg), it fails to explain two key features of the data. First, our observers were sensitive to co-circular pairs across a *wide range* of orientation difference. In the contour detection studies, performance for contours made from orientations that were pairwise co-circular dropped precipitously as the orientation difference  $\theta$  increased from zero, i.e., from the collinear baseline. Our results on the other hand show a slight *increase* in sensitivity from  $\theta$  to a peak at about 45 deg, followed then by only a slight decline. In other words for our textures, co-circularity is a salient feature across a range of orientation difference. This finding is indicative of a fundamental difference between the mechanisms for detecting a contour in noise from those detecting “structure” in a texture; when it comes to detecting texture structure, there appears to be a general preference for angles compared to straight lines (Biederman, 1987; Treisman & Gormican, 1988).

Second, we found a secondary peak in sensitivity for radial co-circular pairs. Although contour detection studies have revealed sensitivity to parallel orientations (May & Hess, 2008), which represent the extreme of radial-type

co-circularity (with performance again falling off sharply as the orientations departed from parallel), our results show a peak in sensitivity for radial co-circular pairs across a range of orientation differences. Again this shows that radial co-circularity is a salient feature across a range of orientation differences.

The present findings suggest a critical role of co-circularity in the perception of textural structures. Co-circularity has been shown to be a fundamental property of edges in natural scenes (Elder & Goldberg, 2002; Geisler, Perry, Super, & Gallogly, 2001; Sigman, Cecchi, Gilbert, & Magnasco, 2001). The sensitivity we have observed for co-circular patterns also explains why textons such as curves and V shapes have long been considered as critical features in texture discrimination. Given the other lines of evidence showing higher sensitivities for global forms (but not textures) such as Glass patterns with concentric or polar structure (Gallant, Braun, & Van Essen, 1993; Wilson & Wilkinson, 1998), sensitivity to co-circularity might be a general property of visual pattern processing.

While we have interpreted the results in terms of the processing of local patterns, sensitivity to co-circularity might reflect the characteristics of a specific mid-level neural representation associated with coding global textures. Recent neuropsychological and fMRI studies suggest the existence of a module specialized for global texture processing in higher visual-cortical areas (Cant, Arnott, & Goodale, 2009; Cant & Goodale, 2007). The stochastic textures employed here could be a useful tool for characterizing such modules in future physiological studies.

## Acknowledgments

This research was supported by McGill-Japan Award.

Commercial relationships: none.

Corresponding author: Isamu Motoyoshi.

Email: motoyosi@apollo3.brl.ntt.co.jp.

Address: 3-1 Morinosato-Wakamiya, Astugi 243-0198, Japan.

## References

- Arsenault, A. S., Wilkinson, F., & Kingdom, F. A. (1999). Modulation frequency and orientation tuning of second-order texture mechanisms. *Journal of the Optical Society of America A, Optics, Image Science, and Vision*, 16, 427–435. [PubMed]
- Barlow, H. B., & Reeves, B. C. (1979). The versatility and absolute efficiency of detecting mirror symmetry in random dot displays. *Vision Research*, 19, 783–793. [PubMed]

- Ben-Shahar, O. (2006). Visual saliency and texture segregation without feature gradient. *Proceedings of the National Academy of Sciences of the United States of America*, 103, 15704–15709. [PubMed] [Article]
- Ben-Shahar, O., & Zucker, S. W. (2004). Sensitivity to curvatures in orientation-based texture segmentation. *Vision Research*, 44, 257–277. [PubMed]
- Bergen, J. R., & Adelson, E. H. (1988). Early vision and texture perception. *Nature*, 333, 363–364. [PubMed]
- Biederman, I. (1987). Recognition-by-components: A theory of human image understanding. *Psychological Review*, 94, 115–147. [PubMed]
- Cant, J. S., Arnott, S. R., & Goodale, M. A. (2009). fMR-adaptation reveals separate processing regions for the perception of form and texture in the human ventral stream. *Experimental Brain Research*, 192, 391–405. [PubMed]
- Cant, J. S., & Goodale, M. A. (2007). Attention to form or surface properties modulates different regions of human occipitotemporal cortex. *Cerebral Cortex*, 17, 713–731. [PubMed]
- Claessens, P. M., & Wagemans, J. (2005). Perceptual grouping in Gabor lattices: Proximity and alignment. *Perception & Psychophysics*, 67, 1446–1459. [PubMed] [Article]
- Claessens, P. M., & Wagemans, J. (2008). A Bayesian framework for cue integration in multistable grouping: Proximity, collinearity, and orientation priors in zigzag lattices. *Journal of Vision*, 8(7):33, 1–23, <http://journalofvision.org/8/7/33/>, doi:10.1167/8.7.33. [PubMed] [Article]
- Dakin, S. C., & Watt, R. J. (1997). The computation of orientation statistics from visual texture. *Vision Research*, 37, 3181–3192. [PubMed]
- Elder, J. H., & Goldberg, R. M. (2002). Ecological statistics of Gestalt laws for the perceptual organization of contours. *Journal of Vision*, 2(4):5, 324–353, <http://journalofvision.org/2/4/5/>, doi:10.1167/2.4.5. [PubMed] [Article]
- Field, D. J., Hayes, A., & Hess, R. F. (1993). Contour integration by the human visual system: Evidence for a local “association field”. *Vision Research*, 33, 173–193. [PubMed]
- Gallant, J. L., Braun, J., & Van Essen, D. C. (1993). Selectivity for polar, hyperbolic, and Cartesian gratings in macaque visual cortex. *Science*, 259, 100–103. [PubMed]
- Geisler, W. S., Perry, J. S., Super, B. J., & Gallogly, D. P. (2001). Edge co-occurrence in natural images predicts contour grouping performance. *Vision Research*, 41, 711–724. [PubMed]
- Glass, L. (1969). Moiré effect from random dots. *Nature*, 223, 578–580. [PubMed]
- Graham, N., Beck, J., & Sutter, A. (1992). Nonlinear processes in spatial-frequency channel models of perceived texture segregation: Effects of sign and amount of contrast. *Vision Research*, 32, 719–743. [PubMed]
- Heeger, D., & Bergen, J. (1995). Pyramid-based texture analysis/synthesis. *Proceedings of ACM SIGGRAPH*, 15, 229–238.
- Hess, R. F., & Dakin, S. C. (1997). Absence of contour linking in peripheral vision. *Nature*, 390, 602–604. [PubMed]
- Julesz, B. (1981). Textons, the elements of texture perception, and their interactions. *Nature*, 290, 91–97. [PubMed]
- Julesz, B., Gilbert, E. N., Shepp, L. A., & Frisch, H. L. (1973). Inability of humans to discriminate between visual textures that agree in second-order statistics—revisited. *Perception*, 2, 391–405. [PubMed]
- Kapadia, M. K., Ito, M., Gilbert, C. D., & Westheimer, G. (1995). Improvement in visual sensitivity by changes in local context: Parallel studies in human observers and in V1 of alert monkeys. *Neuron*, 15, 843–856. [PubMed]
- Kingdom, F. A., Keeble, D., & Moulden, B. (1995). Sensitivity to orientation modulation in micropattern-based textures. *Vision Research*, 35, 79–91. [PubMed]
- Knierim, J. J., & van Essen, D. C. (1992). Neuronal responses to static texture patterns in area V1 of the alert macaque monkey. *Journal of Neurophysiology*, 67, 961–980. [PubMed]
- Landy, M. S., & Bergen, J. R. (1991). Texture segregation and orientation gradient. *Vision Research*, 31, 679–691. [PubMed]
- Locher, P. J., & Wagemans, J. (1993). Effects of element type and spatial grouping on symmetry detection. *Perception*, 22, 565–587. [PubMed]
- Malik, J., & Perona, P. (1990). Preattentive texture discrimination with early vision mechanisms. *Journal of the Optical Society of America A, Optics and Image Science*, 7, 923–932. [PubMed]
- May, K. A., & Hess, R. F. (2008). Effects of element separation and carrier wavelength on detection of snakes and ladders: Implications for models of contour integration. *Journal of Vision*, 8(13):4, 1–23, <http://journalofvision.org/8/13/4/>, doi:10.1167/8.13.4. [PubMed] [Article]

- Nothdurft, H. C. (1985). Sensitivity for structure gradient in texture discrimination tasks. *Vision Research*, 25, 1957–1968. [[PubMed](#)]
- Polat, U., Mizobe, K., Pettet, M. W., Kasamatsu, T., & Norcia, A. M. (1998). Collinear stimuli regulate visual responses depending on cell's contrast threshold. *Nature*, 391, 580–584. [[PubMed](#)]
- Polat, U., & Sagi, D. (1993). Lateral interactions between spatial channels: Suppression and facilitation revealed by lateral masking experiments. *Vision Research*, 33, 993–999. [[PubMed](#)]
- Portilla, J., & Simoncelli, E. P. (2000). A parametric texture model based on joint statistics of complex wavelet coefficients. *International Journal of Computer Vision*, 40, 49–71.
- Sigman, M., Cecchi, G. A., Gilbert, C. D., & Magnasco, M. O. (2001). On a common circle: Natural scenes and Gestalt rules. *Proceedings of the National Academy of Sciences of the United States of America*, 98, 1935–1940. [[PubMed](#)] [[Article](#)]
- Treisman, A., & Gormican, S. (1988). Feature analysis in early vision: Evidence from search asymmetries. *Psychological Review*, 95, 15–48. [[PubMed](#)]
- Wagemans, J., Van Gool, L., Swinnen, V., & Van Horebeek, J. (1993). Higher order structure in regularity detection. *Vision Research*, 33, 1067–1088. [[PubMed](#)]
- Wilson, H. R., & Wilkinson, F. (1998). Detection of global structure in Glass patterns: Implications for form vision. *Vision Research*, 38, 2933–2947. [[PubMed](#)]
- Wolfson, S. S., & Landy, M. S. (1998). Examining edge- and region-based texture analysis mechanisms. *Vision Research*, 38, 439–446. [[PubMed](#)] [[Article](#)]
- Zipser, K., Lamme, V. A., & Schiller, P. H. (1996). Contextual modulation in primary visual cortex. *Journal of Neuroscience*, 16, 7376–7389. [[PubMed](#)]